10th Canadian Masonry Symposium, Banff, Alberta, June 8 – 12, 2005

EXPERIMENTAL STUDY OF THE LATERAL LOAD CAPACITY OF SLENDER, POST-TENSIONED MASONRY WALLS

J.R. Bean[1], A.E. Schultz[2], and C.R. Drake[3]
[1,3]Graduate Research Assistant, Dept. of Civil Engineering, University of Minnesota, USA, bean0032@umn.edu
[2]Associate Professor, Dept. of Civil Engineering, University of Minnesota, 500 Pillsbury Dr. SE, Minneapolis, MN, 55455, USA, schul088@umn.edu

ABSTRACT

An experimental program is described to investigate the behavior of slender, post-tensioned masonry walls to uniformly-distributed, transverse loading (i.e., horizontal loads perpendicular to wall surface, such as wind pressure or earthquake forces). Twelve 3.54 m (11.6-ft) tall walls with 810 x 100 mm nominal (32 x 4 in.) cross-sections were tested under monotonically increasing transverse loads. Six walls were constructed using cored clay brick, and the remaining six using hollow concrete block. The walls were prestressed using threaded post-tensioning bars, and six of the wall specimens featured *unrestrained* tendons (e.g., the cavities containing the tendons were ungrouted and mechanical devices were not used to restrain the tendons), while the other six had *restrained* tendons (e.g., mechanical devices were used to restrain the tendon relative to the masonry). Three different magnitudes of effective prestress were investigated.

The walls were tested vertically in a frame that simulated pinned end conditions, with uniformly distributed lateral load being simulated by a servo-controlled hydraulic force actuator acting through a whiffletree with eight load points at four locations along the wall height. Experimental observations of wall behavior are presented. Maximum deformation capacity of the walls is evaluated in light of these experimental observations.

KEYWORDS: prestressed masonry, post-tensioned masonry, tendon restraint, slender walls, out-of-plane bending, flexural

INTRODUCTION

Post-tensioned masonry walls subjected to lateral loads perpendicular to the surface of the wall have been shown to display two distinct phases of behavior. The first phase is defined by approximately linear elastic response to loading until the wall cracks [1, 2, 3, 4, 5, 6, 7, 8]. The cracking at this point typically occurs at the bed joints when both the compressive stress from the post-tensioning force and the bond strength between the mortar and unit are overcome. Post-cracking behavior, the second phase, features nonlinear load-displacement response until failure [7, 8]. Ultimate strength and failure of the specimen is typically defined by how well the post-tensioned masonry section can maintain its integrity and resist the external forces under increasing compressive strains.

To date, the knowledge concerning the behavior of post-tensioned masonry walls under lateral loading has been derived from the tests on stocky walls (i.e., with low slenderness ratios, *h/t* or *h/r*) [1, 2, 3, 4, 5, 6, 7, 9, 10]. First, the magnitude of prestress primarily impacts the range through which walls are able to maintain elastic behavior [2, 4, 6, 8, 9]. Higher magnitudes of prestress result in higher cracking loads and vice versa. This observation has been found to be similar for walls using different restraint conditions [8]. Also, post-tensioning force affects post-cracking behavior, but here results vary depending upon the restraint condition of the tendon. For walls with restrained tendons, a specimen with a lower magnitude of prestress will typically experience more deformation before reaching its ultimate strength [8]. In a wall with unrestrained tendons, the ultimate strength can be significantly diminished when lower magnitudes of prestress are applied [8].

This discrepancy points out the importance of understanding why walls with restrained and unrestrained tendons behave differently. In walls with restrained tendons, the effective depth of the reinforcement stays constant because the tendons maintain their location within the cross-section. Also, since there is no additional eccentricity of the post-tensioning force due to member deformation, the lack of eccentricity does not contribute to second order effects (i.e., P-Δ effects), which could possibly lead to instability [2, 3, 10]. On the other hand, unrestrained tendons are able to displace within the cross-section and may be susceptible to buckling due to the eccentric positioning of the tendon, which generates P-Δ effects [3, 6, 9, 11]. Overall, the use of restrained tendons is desirable and produces masonry walls that display better post-cracking behavior with improved strength and ductility compared to walls built using unrestrained tendons [3, 5, 6, 7, 12, 13].

Economic pressures are driving the need for masonry walls with considerably high slenderness ratios, and there is concern over the structural safety of these designs, especially in applications with lateral forces of large magnitude. In order to further understand the extent to which slenderness affects post-tensioned masonry walls, an experimental study was conducted at the University of Minnesota. These experiments are part of an ongoing study aimed at analysis and design methods for slender post-tensioned masonry walls.

WALL CONSTRUCTION

The slender, post-tensioned masonry walls designed for this experimental program featured concrete masonry and clay masonry wall panels, with additional features to facilitate testing: header and footer beams, prestressing tendons, tendon restraints, and lateral loading sleeves.

These elements were incorporated into the construction of the concrete and clay wall sections as seen in Figure 1. The experimental research program consisted of testing twelve 3.54-m (11.6-ft) tall walls under monotonically increasing transverse loads. The initial motivation for this study was loading from wind and soil pressure, consequently, monotonic loading was deemed appropriate. Six of the walls were constructed of cored clay brick units, while the remaining six walls were built of concrete block. The concrete masonry walls were face-shell bedded and had a net cross-sectional area of 533 cm^2 (83 in^2), while the clay masonry walls were fully bedded and had a net cross-sectional area of 506 cm^2 (78 in^2). All walls were made using Type S Portland cement-lime mortar, with the compressive strength of the masonry being 12.8 MPa (1860 psi) for the concrete block masonry and 27.0 MPa (3920 psi) for the clay brick.

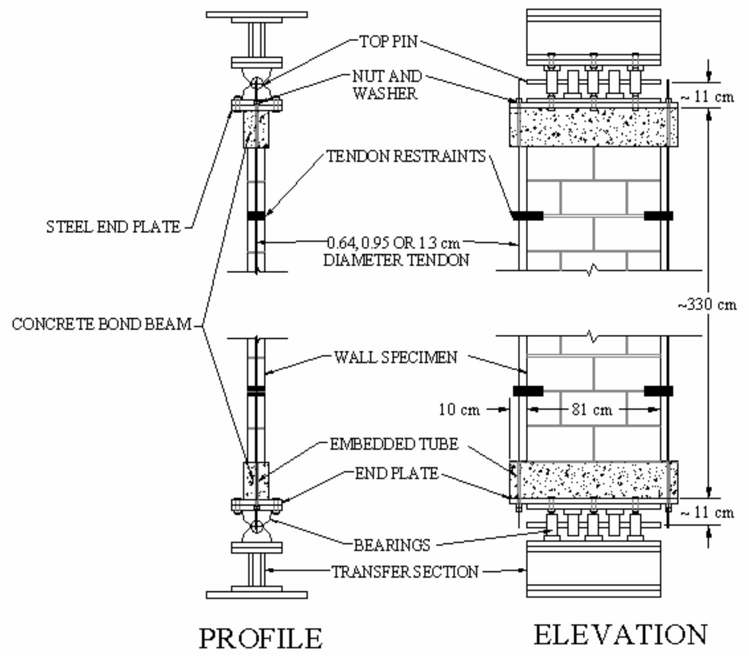

Figure 1 – Vertically-Spanning, Simply-Supported Wall Specimens

The header and footer beams were constructed using a steel plate attached to a concrete bond beam by means of a sand-mortar epoxy, as shown in Figure 1 and 2. These beams gave an equivalent height of a single course of concrete block, as well as three courses of clay bricks. This detail allowed the specimens to be bolted to the pins of the load frame, positioned the post-tensioning bars at the centerline of the wall at the top and bottom, and provided a bearing surface for the post-tensioning bars. Once the specimens were bolted in place and ready to be tested, the resulting pin-to-pin clear height between supports was 3.54-m (139.3–in). Therefore, the final height to thickness ratio (h/t) for these specimens was 38.4 for the concrete block walls and 40.5 for the clay brick walls.

Another variable included in this study was the effective magnitude of prestress that acts on the net cross-sectional area of the wall. Three different magnitudes of prestress were selected for this experimental program, 0.24, 0.52, 1.03 MPa (35, 75, and 150 psi). Each magnitude of prestress was applied to an unrestrained and a restrained wall of each type of masonry. By selecting this range of prestress, it was possible to explore low magnitudes of prestress (e.g., 0.24 and 0.52 MPa), as desired, while also addressing effective magnitudes of prestress that are more applicable in the design of post-tensioned masonry walls (e.g., 1.03 MPa).

As shown in Figure 1 and 2, the prestressing tendons used for all specimens were unbonded ASTM Grade B7 threaded steel bars, which have a tensile strength of 862 MPa (125 ksi) and a yield strength of 724 MPa (105 ksi). Different diameters of threaded rod were used depending upon the effective magnitude of prestress applied to the wall. The diameters were 6.4-mm (1/4-in), 9.5-mm (3/8-in), and 12.7-mm (1/2-in) for prestress magnitudes of 0.24 MPa (35 psi), 0.52 MPa (75 psi), and 1.03 MPa (150 psi), respectively. Two external post-tensioning bars, one on either end, were used to apply the post-tensioning force to every specimen which gave a net cross-sectional area of steel equal to 0.51 cm^2 (0.08 in^2), 1.11 cm^2 (0.17 in^2), and 2.01 cm^2 (0.31

in^2) for the 6.4-mm (1/4-in), 9.5-mm (3/8-in), and 12.7-mm (1/2-in) diameter tendons, respectively. The stress in the tendon was monitored by means of back-to-back strain gauges on couplers placed at discrete locations along the post-tensioning bar. The effective magnitude of prestress on the net area of masonry was brought to the desired magnitude by re-stressing the tendons immediately before testing.

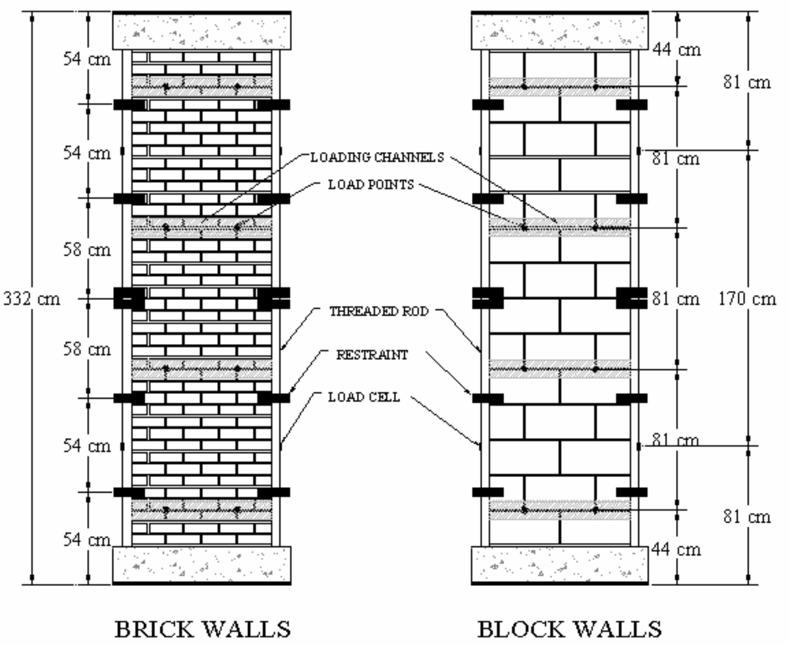

Figure 2 – Specimen Details

The last variable considered was the degree of tendon restraint: six of the wall specimens featured *unrestrained* tendons (e.g., the cavities containing the tendons were ungrouted and mechanical devices were not used to restrain the tendons), while the other six had *restrained* tendons (e.g., mechanical devices were used to restrain the tendon relative to the masonry). Since a target value of 40 was selected for the slenderness ratio (*h*/*t*) of the wall specimens, units of small nominal thicknesses (102-mm or 4-in.) and even smaller cavities (38-mm or 1.5-in.) were required. In order not to restrain the reinforcement in the small cavities of the narrow units, the threaded bars were placed externally on either side of the masonry wall. Moreover, this restraint system allowed for the observation of tendons during out-of-plane loading. Therefore, short lengths of steel tubes were epoxied and bolted on either side of the wall specimen to simulate the inside surface of the masonry cavities, as shown in Figure 1 and 2. The interior dimensions of the external restraints were selected to represent the scaled dimensions of a cavity in a single-wythe wall with 203-mm (8-in.) nominal thickness masonry units. To simulate the restrained condition using these steel tubes, wooden block inserts were fitted inside the tubes to restrict the relative movement of the tendon.

A summary of the experimental variables is given in Table 1.

Table 1 – Experimental Variables

Material		**Magnitude of Prestress**			**Restraint Condition**	
Clay Brick	**Concrete Block**	**0.24 MPa (35 psi)**	**0.52 MPa (75 psi)**	**1.03 MPa (150 psi)**	**unrestrained**	**restrained**
PB1-35-U	PC1-35-U	X			X	
PB2-75-U	PC2-75-U		X		X	
PB3-150-U	PC3-150-U			X	X	
PB4-35-R	PC4-35-R	X				X
PB5-75-R	PC5-75-R		X			X
PB6-150-R	PC6-150-R			X		X

LOADING PROCEDURE

The masonry walls were supported at the top and bottom by spreader beams attached to pins. The bottom pin was attached to the laboratory floor, while the top pin was attached to a steel support beam that was laterally restrained to prevent transverse motion.

The lateral loading applied during the wall tests was generated by a single 155-kN (35-kip) horizontally positioned hydraulic actuator attached to a braced steel column. This loading was delivered to the wall by way of a whiffletree arrangement, which was comprised and assemblage of threaded steel bars, spreader beams, and cylindrical washers. Metal sleeves were located in select bed joints of each wall specimen to facilitate connection to the whiffletree system. Copper tubes were used for the sleeves, which enabled placement of 6.4-mm (1/4-in) threaded bars through the wall to attach loading channels to both faces of the specimen. The loading channels were attached at four locations along a vertical plane using two threaded bars per location, as shown in Figure 2. The placement of the sleeves was such that both the concrete block walls and clay brick walls were loaded at the same elevations. This whiffletree scheme had been used previously [14], and it produced a lateral moment distribution that closely simulated the moment diagram for a uniformly distributed lateral load up to peak load.

The tests were conducted by applying lateral displacement with the horizontal hydraulic actuator through the whiffletree. Lateral displacement at the mid-height of the wall was incremented slowly throughout the test. The loading and specimen response to loading were measured using internal load cells in the actuator, load cells on the whiffletree system, load cells on the post-tensioning bars, and LVDTs at various locations along the height of the masonry.

VISUAL OBSERVATIONS

For all walls, the lateral displacement of the horizontal actuator was increased monotonically as loading was applied. As the lateral loading continued, a horizontal crack opened in a single bed joint at the masonry-mortar interface at or near mid-height, as shown in Figure 3. As testing progressed, the crack width at the opening joint became pronounced and the lateral displacement rapidly increased with subsequent loading. Lateral displacements at the end of loading were significant, on the order of 3 to 5% of wall height, as seen in Figure 4. Furthermore, crushing of the mortar on the compression face of the opening joint was generally observed at mid-height lateral displacement much greater than displacements corresponding to maximum moment capacity.

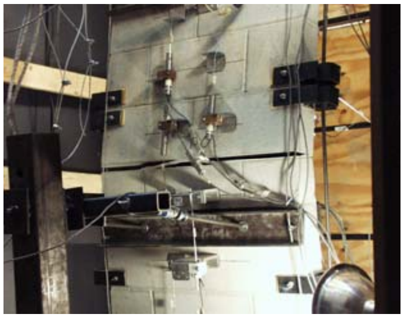

Figure 3 - Photograph of Wall PC6-150-R During Testing

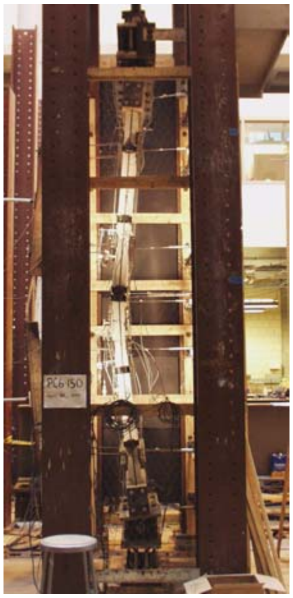

Figure 4 - Profile of PC6-150-R During Testing

MOMENT DISPLACEMENT BEHAVIOUR

A plot of the mid-height moment capacity-displacement response of the specimens can be seen in Figures 5(a) and (b) for the concrete block and clay brick walls, respectively. It was observed that the behaviour of all the specimens prior to cracking was linear-elastic, while the post-cracking behaviour of the wall specimens differed in accordance with the restraint condition of the tendons. It was also noted that the maximum moment was located at some finite (small) distance from mid-height.

The concrete block walls experienced slightly lower moment capacities than the brick walls, which is not surprising given the slightly larger thickness and cross-sectional properties (i.e., area and section modulus) of the block relative to the brick. Moreover, for the lowest magnitude of effective prestress, the post-peak behaviour of the block walls was incrementally more desirable (i.e., less steep unloading branches). Otherwise, no significant differences between the response of the brick and block walls were observed. Also shown in Figure 5, specimens with restrained tendons displayed more controlled behavior after reaching nominal strength. It was further observed that higher magnitudes of effective prestress resulted in higher moment capacities and peak deflections.

Hinge formation controlled the behavior of ten of the twelve walls (PC1-35-U, PC2-75-U, PC3-150-U, PC4-35-R, PB1-35-U, PB2-75-U, PB3-150-U, PB4-35-R, PB5-75-R, and PB6-150-R). Hinge formation refers to an event where a full-width crack penetrated the opening joint and rendered the simply-supported wall a hinged mechanism. All subsequent deformation was concentrated in that plastic hinge. One wall developed a compression failure mechanism (PC6-150-R), where compression failure refers to exhausting the strain capacity of the extreme compression fiber. And, one wall exhibited both hinge formation and compression failure at the instant of maximum moment (PC5-75-R).

TENDON DISPLACEMENT

Two horizontal LVDTs, one connected to each tendon at mid-height, were used to determine the position of the tendons relative to the wall during the lateral load tests. The movement of the tendon with respect to the wall is plotted in Figures 6(a) and (b) for the concrete block and clay brick walls. Tendon relative displacements were not measured during the test of Wall PC5-75-R.

The movement of the tendon in the restrained cases generally coincided with the movement of the wall specimen. Some differential movement for the restrained tendons can be observed, and it is assumed to have originated from two sources. First, the hole for the tendon in the tendon restraint wooden insert was oversized by 1.6-mm (1/16-in.) to allow for the tendons to be installed, which resulted in some displacement until contact with the edge of the hole was made. Moreover, a limited amount of compression of the wooden block insert occurred during testing, but the majority of the measured relative tendon motion was due to tolerance.

The movement of the tendon in the unrestrained cases initiated when lateral loading began. This behaviour indicates that the tendons moved relative to the centerline of the wall section until the tendon come into contact with the inside surface of the restraint at a tendon relative displacement of approximately 2-cm (0.875–in.). Once contact was made, the tendon moved in unison with the wall.

TENDON STRESS HISTORIES

The behaviour of the post-tensioning tendons directly influenced the post-tensioned masonry wall response to lateral loads. Tendon stresses increased during lateral loading, and initiation of this increase corresponded directly to cracking of the specimen. Measured tendon stress histories for the concrete block and clay brick specimens are presented in Figures 7(a) and (b), respectively.

For the unrestrained case, the tendons did not displace laterally, until they came into contact with the inside edge of the restraint. It was also noted that the increase in tendon stress began at the instant of cracking. Prior to cracking, the unrestrained tendons, which were placed at wall mid-depth, coincided with the neutral axis, and elongation was not imposed on the tendon as a result of bending. The neutral axis shift associated with wall cracking resulted in the tendon being located in the tensile region of the wall section, and flexural deformation of the wall resulted in tensile stress change in the tendons. Since the neutral axis continued to shift with increasing lateral displacement, the tendons experienced an increase in tension stress with loading. It can also be noted that the yield strength of the post-tensioning bars was 724 MPa (105 ksi), and stresses in the steel remained well below this limit.

The rate of stress increase in the restrained cases was larger than that of the unrestrained cases. After cracking, the increase in stress in the restrained tendons was larger because the position of the tendons was restricted to the center of the wall section. This caused the neutral axis to shift further from the tendon than in the unrestrained tendons (i.e., tendon eccentricity). For the unrestrained tendons; tendon movement was in the same direction as neutral axis shift (i.e., towards the tension face); which reduced tendon eccentricity.

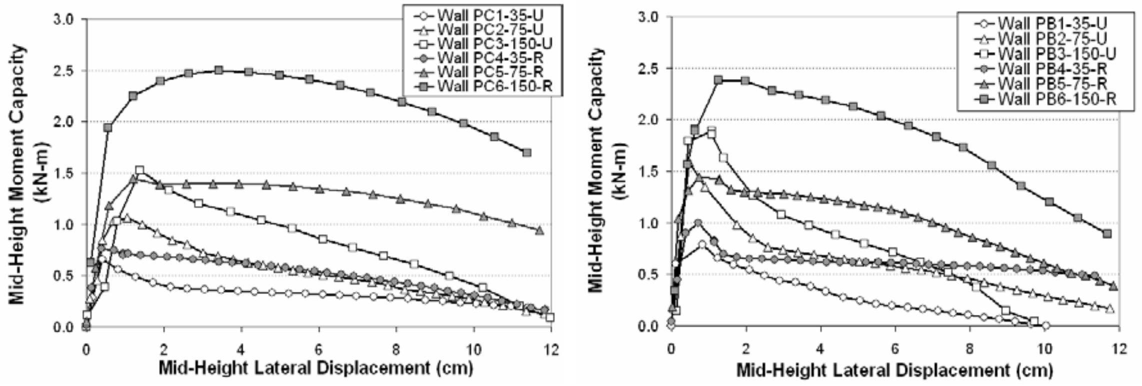

(a) Concrete Block Specimens (b) Clay Brick Specimens

Figure 5 - Experimental Moment - Displacement Behaviour

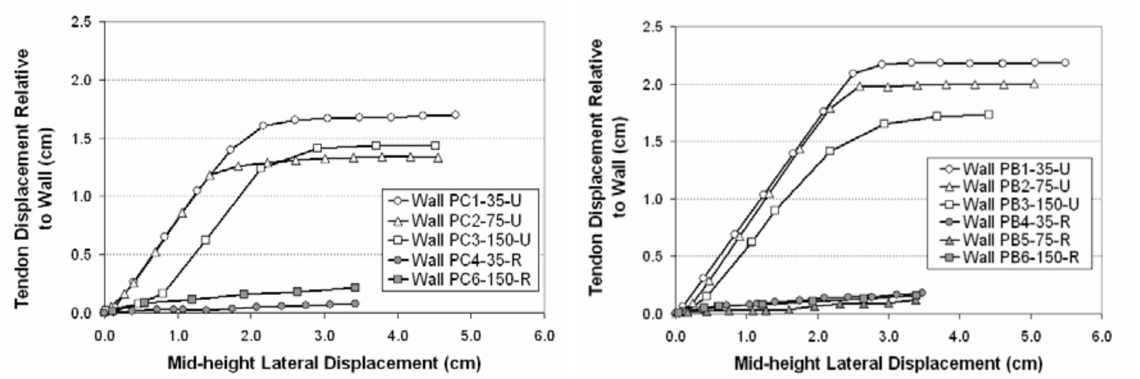

(a) Concrete Block Specimens (b) Clay Brick Specimens

Figure 6 - Tendon Displacement Relative to Wall

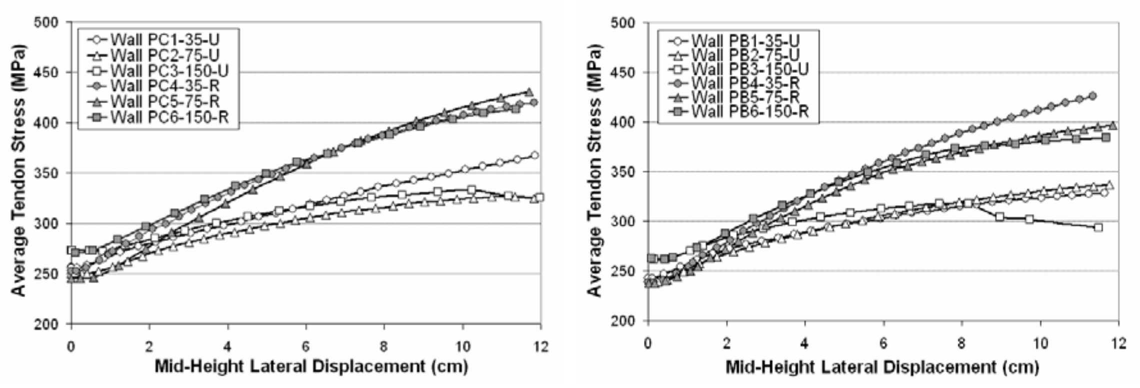

(a) Concrete Block Specimens (b) Clay Brick Specimens

Figure 7 - Experimental Tendon Stress Histories

MEASURED DISPLACEMENTS

Using data from the seven horizontal LVDTs positioned along the height of the wall, displacement profiles at nominal capacity were obtained for the concrete block walls and the clay brick wall, as depicted in Figures 8(a) and (b), respectively. When cracking controlled wall capacity (all brick walls and concrete walls PC1-35-U, PC2-75-U, PC3-150-U, and PC4-35-R), the displacement corresponding to nominal strength was significantly smaller than when the walls failed in compression (concrete walls PC5-75-R and PC6-150-R). Additionally, wall specimens with higher magnitudes of effective stress sustained higher displacements.

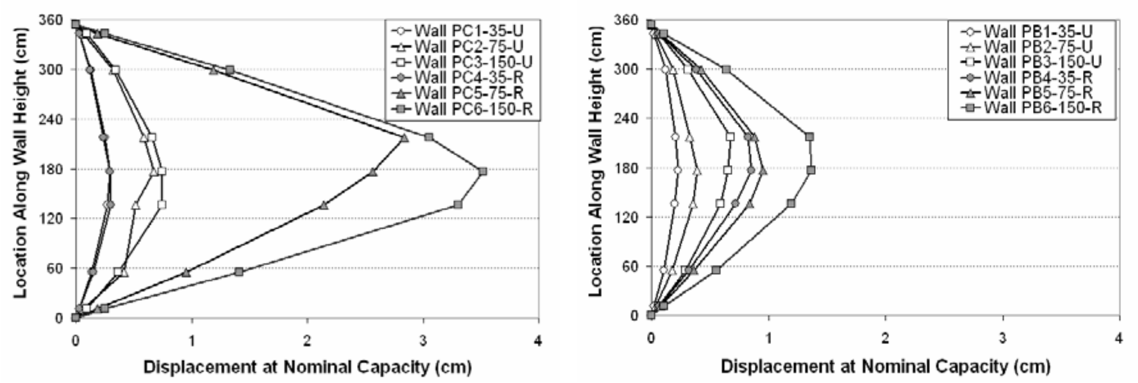

(a) Concrete Block Specimens (b) Clay Brick Specimens

Figure 8 - Displacement Profiles of the Wall Specimens at Moment Strength

COMPARISON OF DRIFT CAPACITIES

Although moment capacity of post-tensioned masonry walls is an important aspect, so too is the deformation capacity. For this study, the deformation capacity was defined as the mid-height displacement when moment capacity drops to 80% of the peak (measured) strength. The drift ratio for each wall specimen was calculated as the ratio of deformation capacity to one-half of the pin-to-pin wall height. This corresponding drift ratios were 0.6%, 1.3%, 1.5%, 2.5%, 6.0%, 5.8%, 0.5%, 0.6%, 0.8%, 0.7%, 2.5%, and 3.7%, respectively, for Walls PC1-35-U, PC2-75-U, PC3-150-U, PC4-35-R, PC5-75-R, PC6-150-R, PB1-35-U, PB2-75-U, PB3-150-U, PB4-35-R, PB5-75-R, PB6-150-R. Thus, walls with a higher effective magnitude of prestress and restrained tendons exhibited more deformation capacity than did walls with lower prestress and unrestrained tendons. Additionally, it was observed that when lateral loading was removed, all walls displayed self-righting behaviour (i.e., cracked joints closed and deflections vanished).

CONCLUSION

All of the wall specimens underwent large displacements before losing their load carrying capacity, with maximum mid-height displacements ranging from 3 to 5% total wall height (i.e., pin-to-pin). The nature of wall response to lateral load, as indicated by the shape of the moment-displacement curves, depended upon the magnitude of prestress, the restraint condition of the tendons, and the type of masonry. Generally, walls with larger magnitudes of prestress performed better than those with smaller prestress magnitudes: they exhibited larger moment capacities and lesser sensitivity to cracking (i.e., smaller fluctuations in moment capacity upon cracking) than the walls with smaller magnitudes of prestress. Walls with restrained tendons exhibited a better response than those with unrestrained tendons, as they displayed slower rates of strength degradation after reaching peak capacity.

ACKNOWLEDGEMENTS

Financial support was provided by the National Concrete Masonry Assoc. (NCMA) Foundation, the Brick Industry Assoc. (BIA), and the International Masonry Inst. (IMI), the US National Science Foundation (NSF) through grant CMS-9904110, and the University of Minnesota. Materials and labor were donated by the Anchor Block Co., Minnesota Brick & Tile Co., Sika Corp., and the *Bricklayers and Allied Craft Workers Local Union 1*, Minneapolis, Minnesota.

REFERENCES

1. Al-Manaseer, A. A. and Neis, V. V. (1987). "Load tests on post-tensioned masonry wall panels." *ACI Structural Journal*, 84(6), 467-472.
2. Geshwinder, L. F. and Ostag, W. P. (1990). "Post-tensioned single wythe concrete masonry walls." *Proc.*, *5th North American Masonry Conference*, Urbana-Champaign, Illinois, 1123-1134.
3. Ungstad, D. G., Hatzinikolas, M. A. and Warwaruk, J. (1990). "Prestressed concrete masonry walls." *Proc.*, *5th North American Masonry Conference*, Urbana-Champaign, Illinois, 1147-1161.
4. Dawe, J. L. and Aridru, G. G. (1992). "Post-tensioned concrete masonry walls subjected to uniform lateral loadings." *Proc.*, *6th Canadian Masonry Symposium*, Saskatoon, Saskatchewan, 201-212.
5. Devalapura, R. K. (1995). "Development of prestressed clay brick masonry walls." Ph.D. Thesis, University of Nebraska, Lincoln.
6. Graham, K. J. and Page, A. W. (1995). "The flexural design of post-tensioned hollow clay masonry." *Proc.*, *7th Canadian Masonry Symposium*, Hamilton, Ontario, 763-774.
7. Rodriguez, R., Hamid, A. A. and Larralde, J. (1998). "Flexural behavior of post-tensioned concrete masonry walls subjected to out-of-plane loads." *ACI Structural Journal*, 95(1), 61-70.
8. Drysdale, R. G., Hamid, A. A. and Baker, L. R. (1999). *Masonry Structures: Behavior and Design*, Second Edition, The Masonry Society, Boulder, Colorado.
9. Lacika, E. M. and Drysdale, R. G. (1995). "Experimental investigation of slender prestressed brick walls." *Proc.*, *7th Canadian Masonry Symposium*, Hamilton, Ontario, 724-735.
10. Mojsilovic, N. and Marti, P. (1996). "Load tests on post-tensioned masonry walls." *Proc.*, *7th North American Masonry Conference*, South Bend, Indiana, 327-335.
11. Walkowicz, S. W. (2003). "Post-tensioning case histories," *Proc., 9th North American Masonry Conference*, Clemson, South Carolina, 499-510.
12. Schultz, A. E. and Scolforo, M. J. (1991). "An overview of prestressed masonry." *The Masonry Society Journal*, 10(1), 6-21.
13. Stierwalt, D. D. and Hamilton, H. R., III (2000). "Restraint effectiveness in unbonded tendons for prestressed masonry," *ACI Structural Journal*, 97(6), 840-848.
14. Bean, J.R. (2003). "Experimental Verification of the Resistance of Masonry Walls under Transverse Loads." M.S. Thesis, University of Minnesota.